atmosphere

MDPI

Article

Spatial Recognition of Regional Maximum Floods in Ungauged Watersheds and Investigations of the Influence of Rainfall

Nam-Won Kim [1], Ki-Hyun Kim [2] and Yong Jung [2,*]

[1] Water Resources Research Division, Water Resources and Environment Research Department, Korea Institute of Construction Technology, Goyang 10228, Korea; nwkim@kict.re.kr
[2] Department of Civil and Environmental Engineering, Wonkwang University, Iksan 54538, Korea; hlkh92@gmail.com
* Correspondence: yong_jung@wku.ac.kr

Abstract: This study primarily aims to develop a method for estimating the range of flood sizes in small and medium ungauged watersheds in local river streams. In practice, several water control projects have insufficient streamflow information. To compensate for the lack of data, the streamflow propagation method (SPM) provides streamflow information for ungauged watersheds. The ranges of flood sizes for ungauged watersheds were generated using a specific flood distribution analysis based on the obtained streamflow data. Furthermore, the influence of rainfall information was analyzed to characterize the patterns of specific flood distributions. Rainfall location, intensity, and duration highly affected the shape of the specific flood distribution. Concentrated rainfall locations affected the patterns of the maximum specific flood distribution. The shape and size of the minimum specific flood distribution were dependent on the rainfall intensity and duration. The Creager envelope curve was used to generate equations for the maximum/minimum specific flood distribution for the study site. The ranges of the specific flood distributions were produced for each watershed size.

Keywords: ranges of flood sizes; specific flood distributions; ungauged watersheds; influence of rainfall characteristics

Citation: Kim, N.-W.; Kim, K.-H.; Jung, Y. Spatial Recognition of Regional Maximum Floods in Ungauged Watersheds and Investigations of the Influence of Rainfall. *Atmosphere* **2021**, *12*, 800. https://doi.org/10.3390/atmos12070800

Academic Editors: Jong-Suk Kim, Nirajan Dhakal, Changhyun Jun and Taesam Lee

Received: 4 May 2021
Accepted: 16 June 2021
Published: 22 June 2021

1. Introduction

Streamflow data is fundamentally required for the flood design process in water control projects. Many water control infrastructures are built in small/mid-sized regional watersheds, which require records of maximum floods. However, there are scarce observed streamflow data for small-and mid-sized watersheds. Most streamflow observations are obtained at hydrologically interesting locations or at the end of a large watershed located downstream. Many studies estimate maximum regional floods using observed data through various approaches, including empirical, deterministic, and probabilistic methods [1]. Several empirical studies have used regional extreme flood records for empirical flood estimations and other related analyses (e.g., Kovacs [2]: 30 sites at South Africa; Acreman [3]: UK floods for 200-year records; Furey and Gupta [4,5]: data from Goodwin Creek experimental watersheds; Patnaik et al. [6]: 358 basins from the USGS database). For other approaches, rational formulas and flood frequency analyses in deterministic and probabilistic methods also used observed data.

However, many countries, especially developing countries, have limited records of large floods [7]. To overcome this, streamflow data for ungauged watersheds were generated by regionalization or regression analysis [8]. Regionalization used streamflow data near watersheds that have similar characteristics (e.g., physiographic and meteorological features) by transferring streamflow data to ungauged watersheds [9–11]. The regression method was used to search for relationships between streamflow data and watershed characteristics and generate streamflow data for ungauged watersheds [12–14]. As a modified regionalization method, Kim et al. [15] suggested a robust method (i.e., streamflow

propagation method (SPM)) to generate streamflow data for ungauged small/mid-sized watersheds. Unlike other regionalization methods, this study aimed to minimize uncertainties using fixed, physically related parameters, while an initial condition (i.e., initial soil saturation) was optimized in a simple lumped conceptual rainfall-runoff model.

In contrast to limited streamflow information, the generated streamflow data can display the spatial distribution of streamflow data for various sizes of watersheds. In this study, we attempt to obtain the ranges of maximum regional floods to aid in the management of small and mid-sized watersheds (less than ~2500 km^2) for which no streamflow data exist. Additionally, the spatial distribution of streamflow for ungauged watersheds and rainfall characteristics on these distributions are explored to generate a range of streamflow magnitude for various sizes of watersheds. The dynamics of rainfall (e.g., rainfall intensity and duration) have substantial effects on the structure of peak discharge [16]. The remaining sections of this paper are organized as follows: Section 2 provides a methodology of this study and Section 3 explains the concept of the streamflow propagation method (SPM) and the study area with selected storm events. The results of streamflow propagation and rainfall effects on the streamflow distribution are presented in Section 4, and Section 4 concludes the study.

2. Methodology

To know the ranges of flood sizes in small- and mid-sized watersheds requires an extensive amount of streamflow data. However, smaller-sized watersheds have a lack of streamflow information frequently due to an abundant amount of timely and economical expenses for monitoring. Thus, the SPM [15] was adopted to generate streamflow data for ungauged smaller watersheds. Kim et al. [15] suggested the spatial propagation of streamflow data using a lumped conceptual model to generate streamflow data for ungauged watersheds. Spatial propagation is achieved when a rainfall-runoff model is run to match the observed streamflow data. Simulations of a rainfall-runoff model for a large watershed can simultaneously produce streamflow information for smaller watersheds within this large watershed. However, several parameters optimized for the simulation can produce many uncertainties in the generated streamflow data [16]. Therefore, a minimum number of parameters were selected for this propagation process to reduce uncertainties as far as possible. The propagation shares a similar magnitude of error Equation (1) to ungauged watersheds within a large watershed, while a rainfall-runoff model attempts to fit streamflow data. In their study, Kim et al. [15] applied the storage function method [17] as a rainfall-runoff model. The model parameters were separated into two sets: physically based parameters and time-variant (i.e., event-based) initial conditions. The physically based parameters highly related to the characteristics of watersheds are fixed, while initial conditions are optimized to fit the streamflow data. This separation provides errors similar to those of gauged watersheds to ungauged watersheds in the propagation process. The substantial differences between this method and the regular regionalization methods are the separation of parameters and focused time for simulations (i.e., not for the prediction but for the past data generation), as shown in Figure 1.

$$\varepsilon_i = \left(\frac{O_i - S_i}{O_i} \right)^2, \; where \; i = 1, \; 2, \; \ldots, \; n \tag{1}$$

$$\varepsilon_1 \cong \varepsilon_2 \cong \ldots \cong \varepsilon_n$$

where ε_i is the error rate at watershed i, and O_i and S_i are the observed and simulated streamflow values at watershed i, respectively.

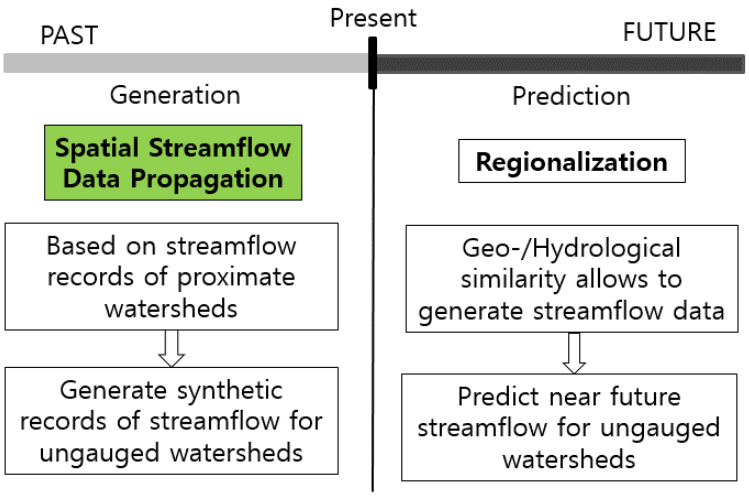

Figure 1. Comparison between the spatial propagation concept and regionalization [15].

After streamflow data generation, streamflow distributions for various sizes of watersheds were observed by using a specific flood distribution analysis, which was usually used to display the streamflow rate for each rainfall event. In this study, we apply this method to display the possible ranges of streamflow amount for the diverse sizes of watersheds. After obtaining the ranges of streamflow, two research questions are addressed: the influence of rainfall on the streamflow distribution and the possible generalization of the range of the streamflow distribution using envelop curve equations to represent (Figure 2). The influence of various rainfall characteristics (e.g., rainfall location, intensity, and duration) was investigated on the effects of the distribution of streamflow for smaller watersheds. For a generalized representation of the range of streamflow distribution (i.e., maximum/minimum specific floods), Creager's envelop curves [18], Kovacs' regional maximum flood [2], and the Korean regional maximum flood equation (KRMF) [19] were tested. The equations of Creager's envelop curves, Kovacs' regional maximum flood, and the KRMF are presented in Equations (2)–(4), respectively.

$$q = 0.503C(0.3861A)^{(aA^b-1)} \tag{2}$$

where q is the specific flood ($m^3/s{\cdot}km^2$), C is the Creager coefficient, A is Area (km^2), and a and b are constant variables.

$$Q = 10^6\left(\frac{A}{10^8}\right)^{1-0.1K} \tag{3}$$

where Q is the streamflow (m^3/s), A is the area (km^2), and K is the coefficient (representing the characteristics of watersheds).

$$q = 11.25\frac{1}{A^{0.25}} \tag{4}$$

where q is the specific flood ($m^3/s{\cdot}km^2$), and A is the area (km^2).

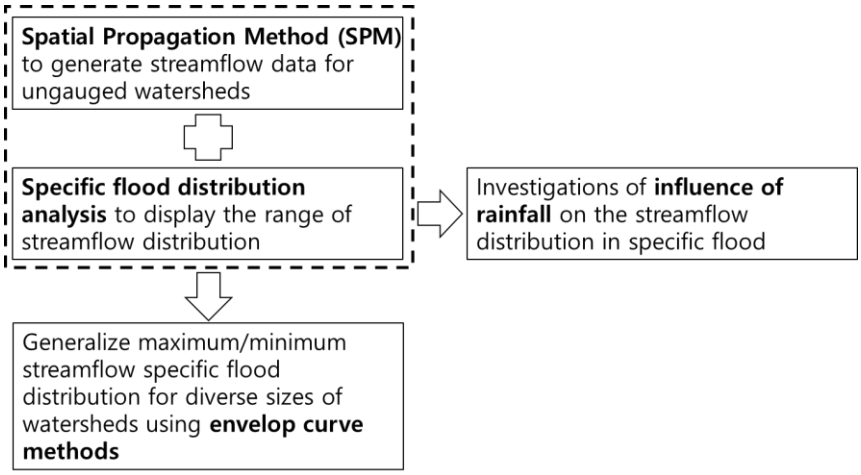

Figure 2. Methodology to represent the range of the streamflow distribution and additional studies related to the specific flood distribution.

3. Study Area and Storm Events

The Han River basin, located near the center of the Korean peninsula, has two major streams: the Northern and Southern Han River streams. The Chungju Dam (CJD) watershed for the study site is located in the upstream part of the Southern Han River stream. The size and length of the CJD watershed are approximately 6648 km^2 and 375 km, respectively. The average width downstream of the CJD is 600 m, with an increased average slope of streamflow. The CJD has a 40% slope for 55.1% of the watershed, and 8.3% of the watershed has a slope of over 80%, meaning that the CJD watershed is located in a mountainous area. Figure 3 shows a streamflow schematic of the CJD watershed. The CJD watershed has two main streams, the left and right sides of the watershed, combined in the middle of the watershed. In this study, the CJD watershed was divided into 35 smaller watersheds with no streamflow information available. To determine the spatial properties of maximum regional floods for a large watershed, spatially distributed streamflow data are necessary. However, most smaller watersheds have limitations in providing streamflow information, as previously mentioned in the Introduction. In the case of the CJD watershed, 12 streamflow gauge stations are insufficient to present the spatial characteristics of the regional maximum flood. Therefore, a propagation process is necessary. We used four different water level gauges (i.e., Chungju Dam (CJD), Youngwol (YW), Youngwol 1 (YW1), and Youngchun (YC)) as validation points, as shown in Figure 3. The CJD inflow was the primary information we wanted to match, while streamflow data propagated to smaller watersheds. The CJD watershed has a significant amount of rainfall during the summer season from June to August, most likely over 60% of the total rainfall. For this study, 18 events with maximum rainfall were selected from 2001 to 2018, as shown in Table 1.

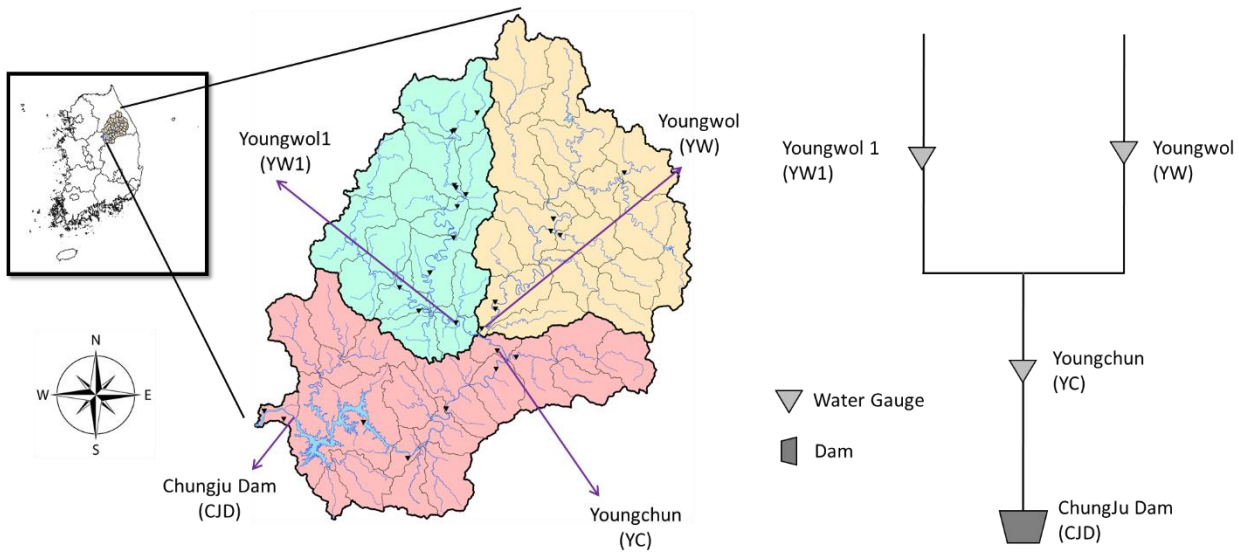

Figure 3. Chungju Dam watershed for study area with two major upstream flows and one combined downstream flow.

Table 1. Selected storm events for CJD watershed.

Event	Start	End	Total Rainfall (mm)	Event	Start	End	Total Rainfall (mm)
1	2001/6/29 0:00	2001/7/4 0:00	101.88	10	2010/9/10 0:00	2010/9/15 0:00	150.33
2	2002/8/6 0:00	2002/8/10 0:00	375.94	11	2011/8/16 0:00	2011/8/19 0:00	145.78
3	2003/7/8 0:00	2003/7/13 0:00	79.86	12	2012/7/5 0:00	2012/7/8 0:00	184.17
4	2004/7/11 0:00	2004/7/15 0:00	136.64	13	2013/7/14 0:00	2013/7/17 0:00	163.16
5	2005/7/1 0:00	2005/7/3 0:00	102.42	14	2014/8/17 0:00	2014/8/23 0:00	106.44
6	2006/7/14 0:00	2006/7/20 0:00	441.94	15	2015/8/24 0:00	2015/8/29 0:00	53.65
7	2007/8/4 0:00	2007/8/7 0:00	126.01	16	2016/7/4 0:00	2016/7/8 0:00	227.03
8	2008/7/24 0:00	2008/7/29 0:00	197.40	17	2017/7/2 0:00	2017/7/6 0:00	190.55
9	2009/7/12 0:00	2009/7/14 0:00	142.90	18	2018/7/1 0:00	2018/7/5 0:00	136.79

4. Results and Discussion

4.1. Generation of Streamflow Data

In the application of a lumped conceptual model (i.e., t storage function method, Kimura 1961) for propagation, there are two parameter sets: physically based parameters (k and p: constant parameters, T_l: lag time) and event-based parameters (f_1: initial runoff ratio, R_{sa}: cumulative saturated rainfall). For the process presented in Figure 4, the cumulative saturated rainfall (R_{sa}) was optimized with an objective function based on the Nash–Sutcliffe efficiency (NSE) at the CJD gauge point while other parameters were fixed. This method delivers a similar magnitude of error for all smaller watersheds. Figure 5 shows the finalized data propagation results using error rates at the validation points. When the soil is fully saturated, the cumulative saturated rainfall is 0, thus suggesting that all rainfall will be fully effective rainfall. The zero cumulative saturated rainfall at events 5, 6, and 9 had previous rainfall events. In terms of error rates, the exit points (i.e., CJD inflow observatory from upstream watersheds) showed higher values at events 3 and 8. The observed values at the CJD increase sharply without any smoother patterns, as shown by other observation points, which means that observations were possibly measured incorrectly. In event 15, the YC and YW have higher error rates because observations at the YC and YW malfunctioned to produce flat values from the beginning of the event (e.g., 34.22 m^3/s at the YC and 34.51 m^3/s at the YW) until a certain point of measurement time, then abruptly increased to the peak streamflow. In addition to these events, Figure 5 shows that the streamflow propagation follows the assumption that similar magnitudes of error rates were distributed, as mentioned in Section 2.

Figure 6 shows the comparisons between the observed and simulated streamflow and peak streamflow at YW, YW1, and YC, respectively. The YC gauge station located below YW1 and YW showed larger streamflow values. The streamflow values at YW were underestimated, while those of YW1 were overestimated. These two contrasting results compensate each other, and the simulated results at the YC show closer streamflow values to the observations because the YC is located under the YW and YW1 gauge stations. The possible reason for contrasting streamflow estimations is the various times of concentration related to the slopes of directions of the YW1 and YW. The fixed parameters are not adjustable based on the status of smaller watersheds in the SPM. The NSEs for peak streamflow at YW1, YW, and YC were 0.94, 0.88, and 0.89, respectively.

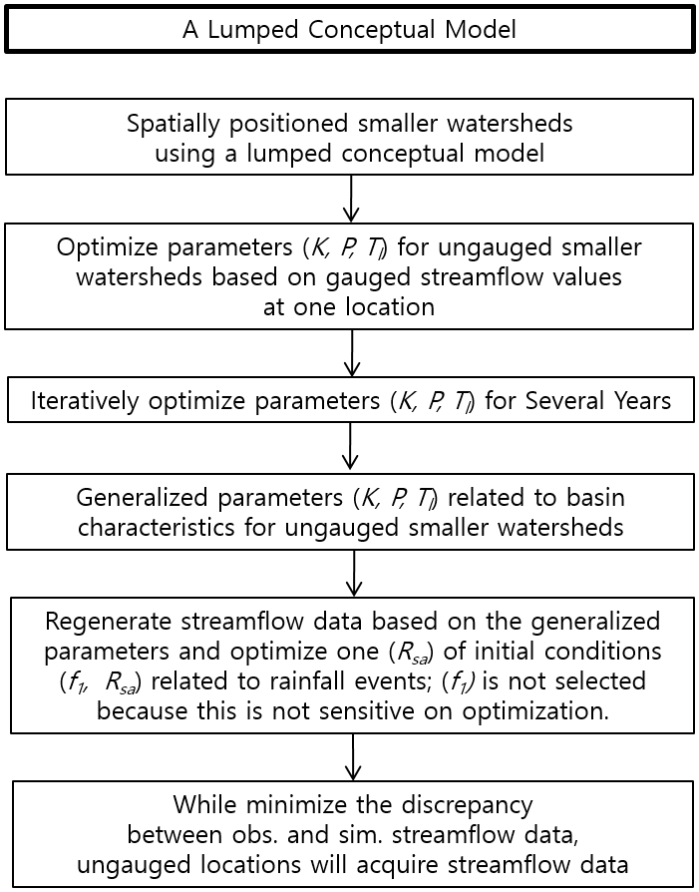

Figure 4. Spatial propagation procedure [15].

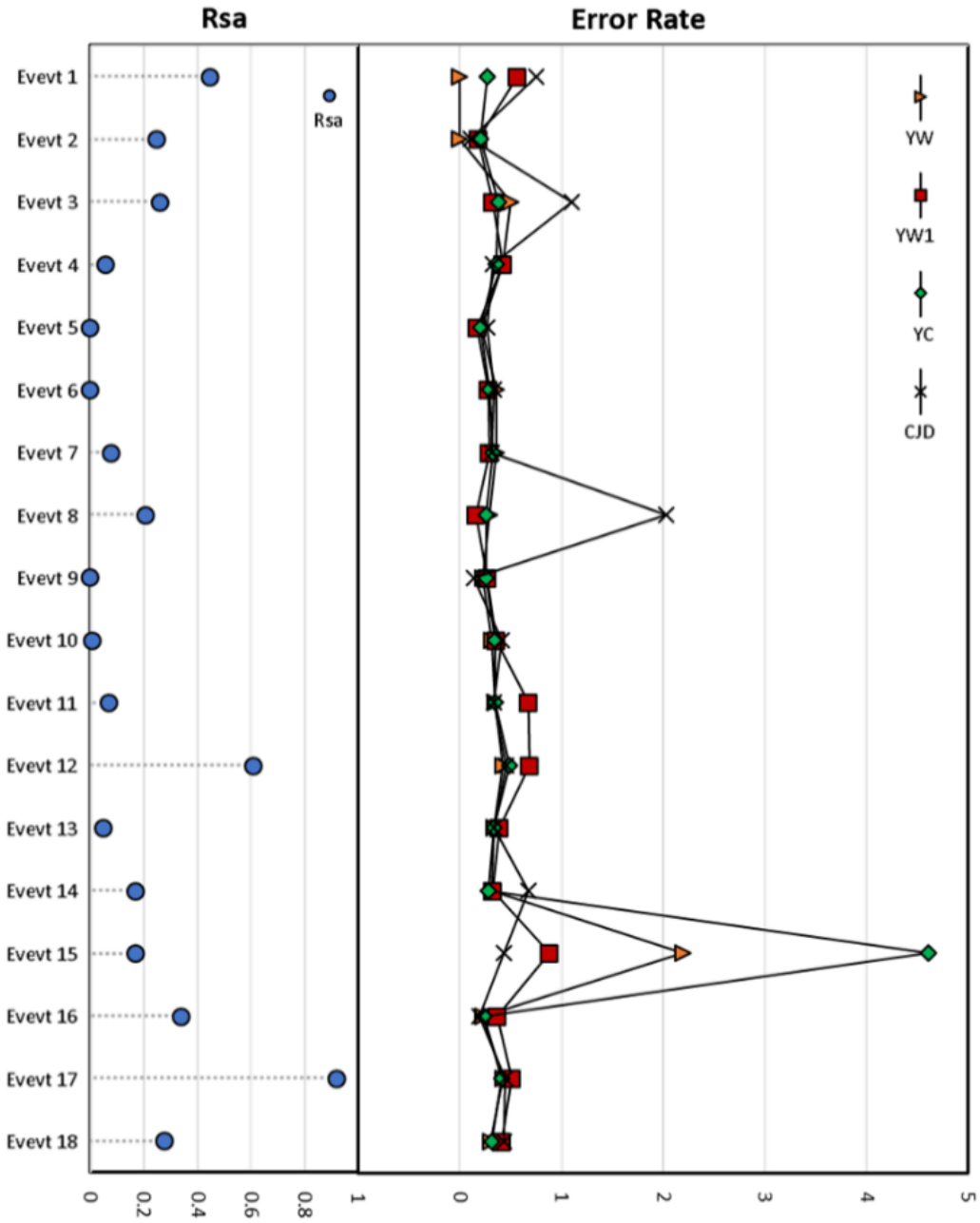

Figure 5. Cumulative saturated rainfall (R_{sa}) and error rates of streamflow data propagation at each gauge station (YW: Youngwol, YW1: Youngwol 1, YC: Youngchun, and CJD: Chungju Dam). Events' details displayed in Table 1.

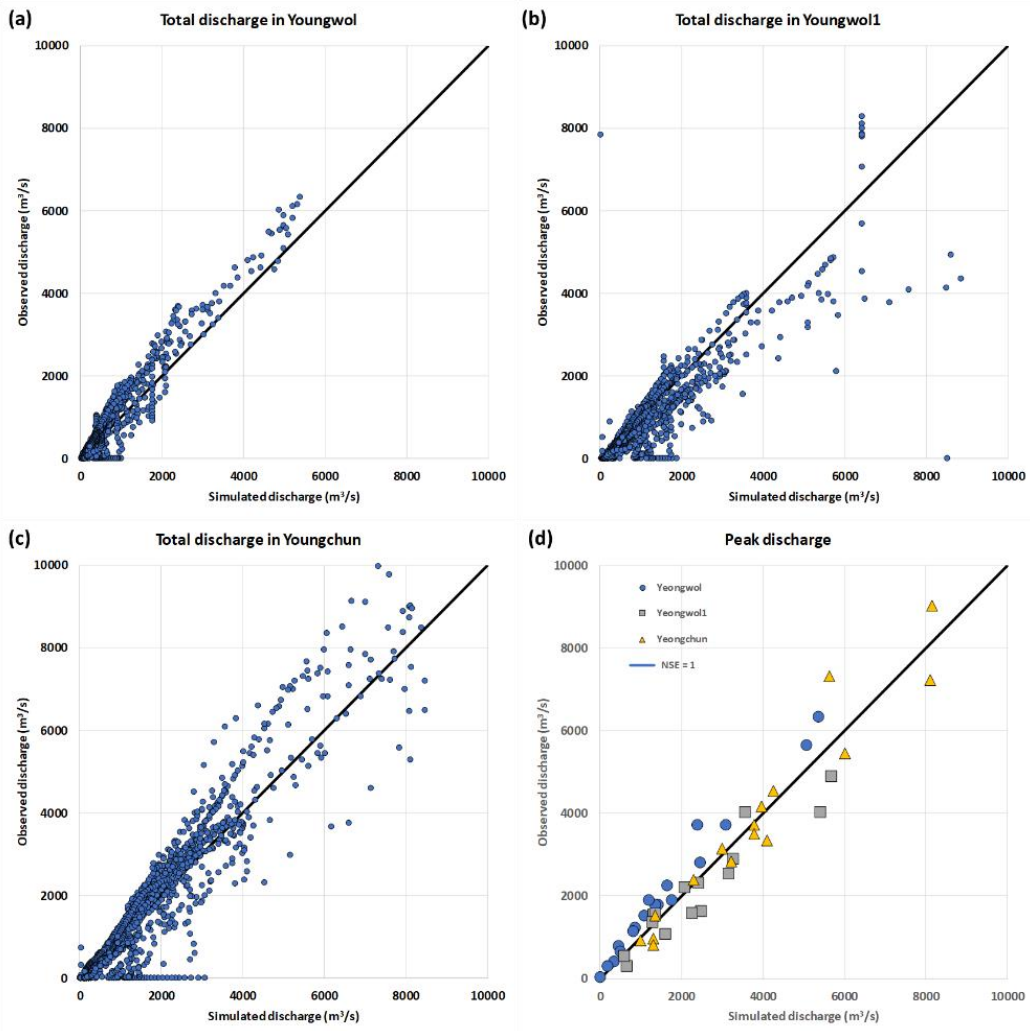

Figure 6. Comparison between observed and simulated peak streamflow values at propagated points. (**a**–**c**) all discharge comparisons at YW, YW1, and YC, (**d**) peak discharge comparisons.

4.2. Effects of Rainfall on Specific Floods

4.2.1. Rainfall Locations

In this study, a specific flood diagram was adopted to show the rainfall intensities on similarly sized watersheds and display the spatial patterns of streamflow based on the diverse sizes of watersheds. With only observed streamflow data, the patterns of specific floods are barely distinguishable; however, propagated streamflow data may enhance the type of spatial streamflow patterns. The patterns of the spatial distributions of streamflow are validated in Figures 7–9. The spatial distribution of streamflow is highly dependent on rainfall distribution [7]. When rainfall is concentrated on upstream watersheds (i.e., watershed 21, or watersheds 1 and 2, which are highlighted in Figure 7 with watershed numbers) with 20 mm/h (other watersheds with 10 mm/h rainfall) for 24 h, the patterns of the specific flood have power–law profiles, as shown in Figure 7a,b, between specific flood and watershed areas; this has been confirmed by the empirical results of existing research [20–22]. Small watersheds located in the same stream lines displayed as red dots in Figure 7a,b form the power–law pattern in a specific flood. In addition to the power–law patterns, equally distributed rainfall (10 mm/h) has a linearly distributed specific flood below the power–law patterns. In the case of concentrated rainfall downstream (i.e., watershed 32) as shown in Figure 7c, there are no substantial effects for the power–law patterns because the concentrated rainfall location is on downstream watersheds.

Figure 7d displays a sample of specific floods based on the observed rainfall data (event 2013). This specific flood pattern shows the horn shape of the specific flood distribution with a power-law, which means that rainfall was concentrated at upstream watersheds and well distributed with diverse sizes of rainfall.

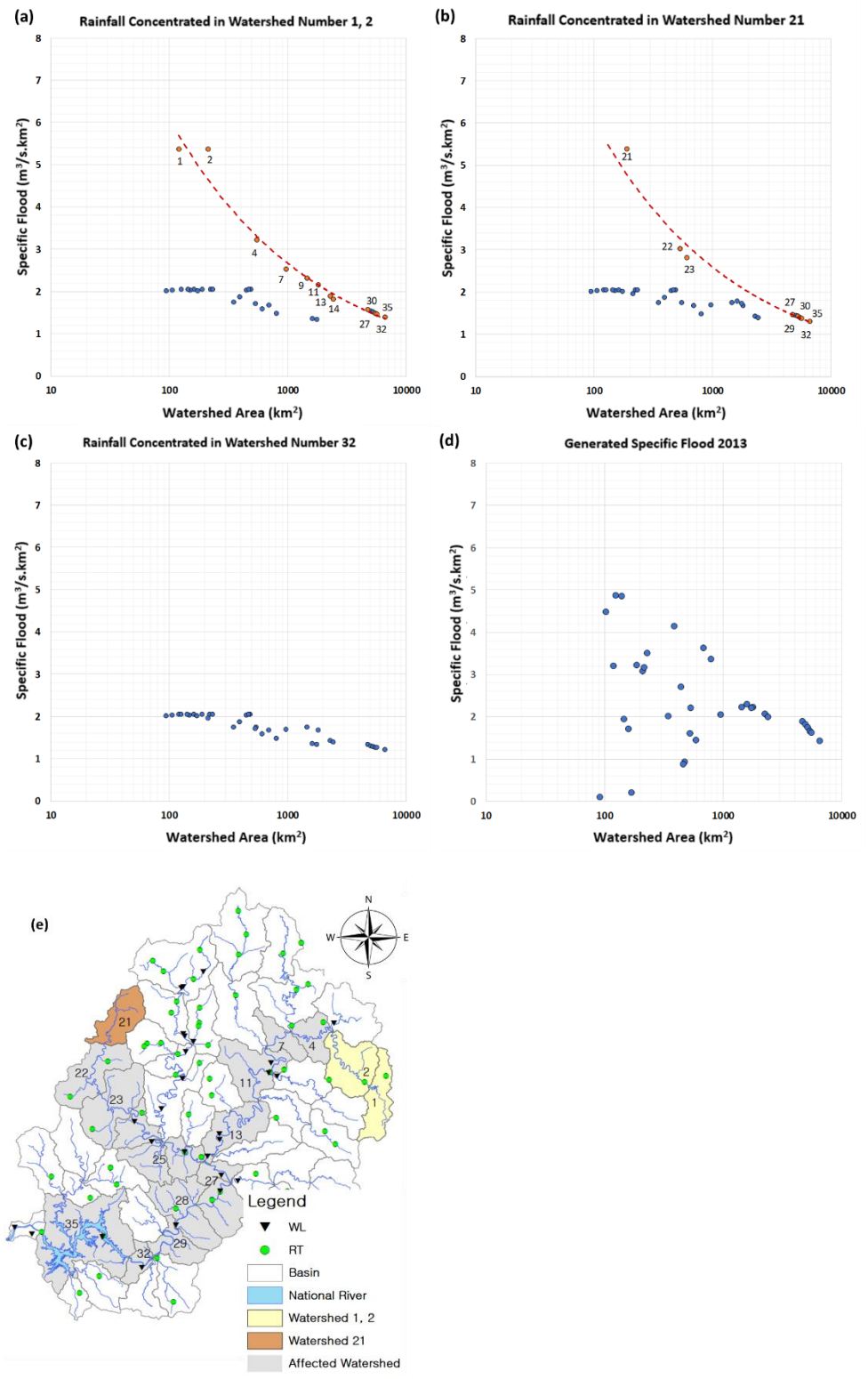

Figure 7. Power–law patterns based on the rainfall concentrated locations (**a**) upstream watershed 21, (**b**) upstream watersheds 1 and 2, (**c**) downstream watershed 32, (**d**) rainfall patterns for an event in 2013), (**e**) concentrated rainfall at watershed 21 (20 mm/hr) or watersheds 1 and 2 (20 mm/hr), with consistent rainfall at other watersheds (10 mm/hr).

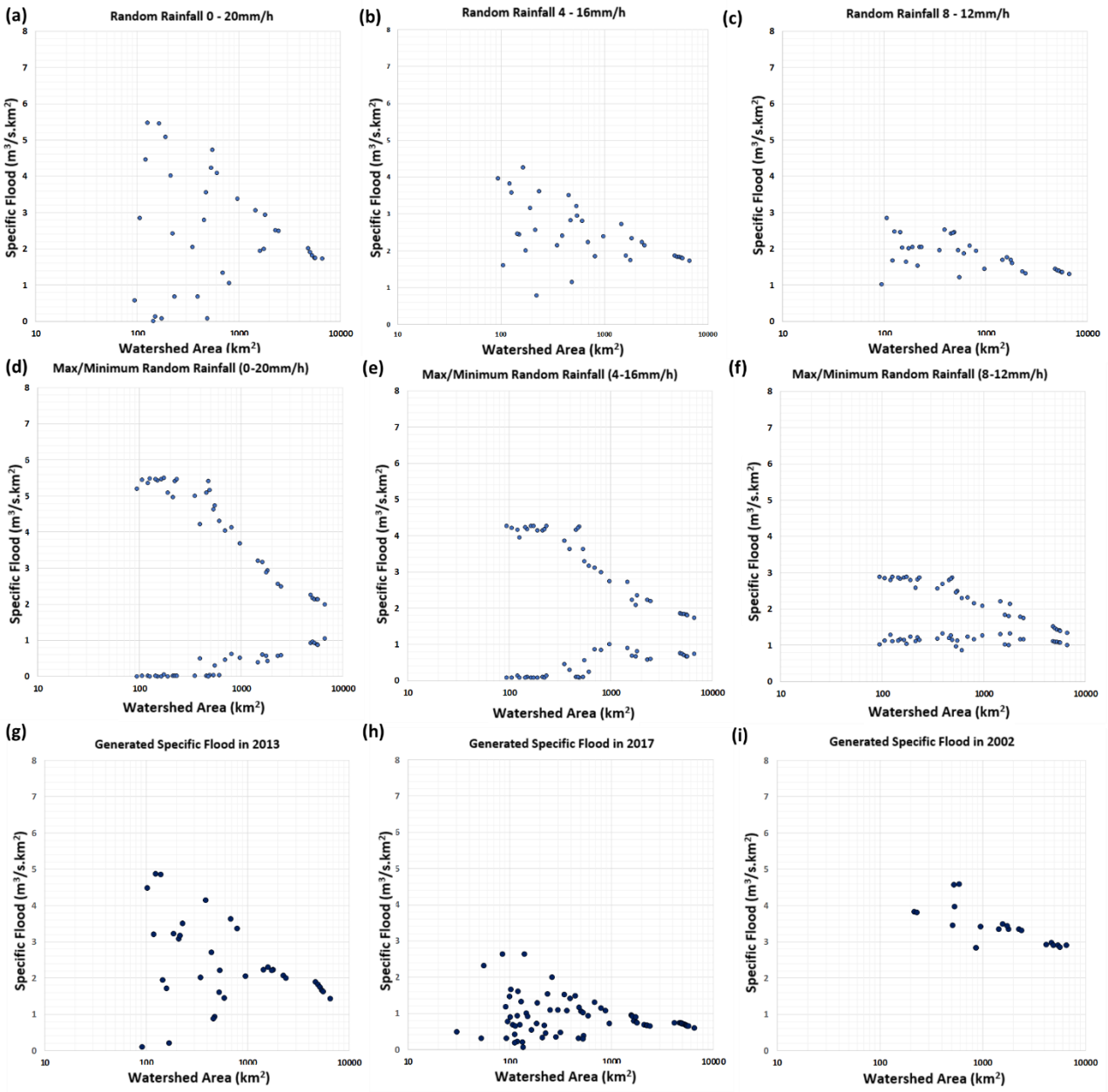

Figure 8. Specific flood based on the different size of rainfall distribution ((**a**–**c**) Simulation cases, (**d**–**f**) maximum and minimum size collection of specific floods for 30 trials, (**g**–**i**) real cases).

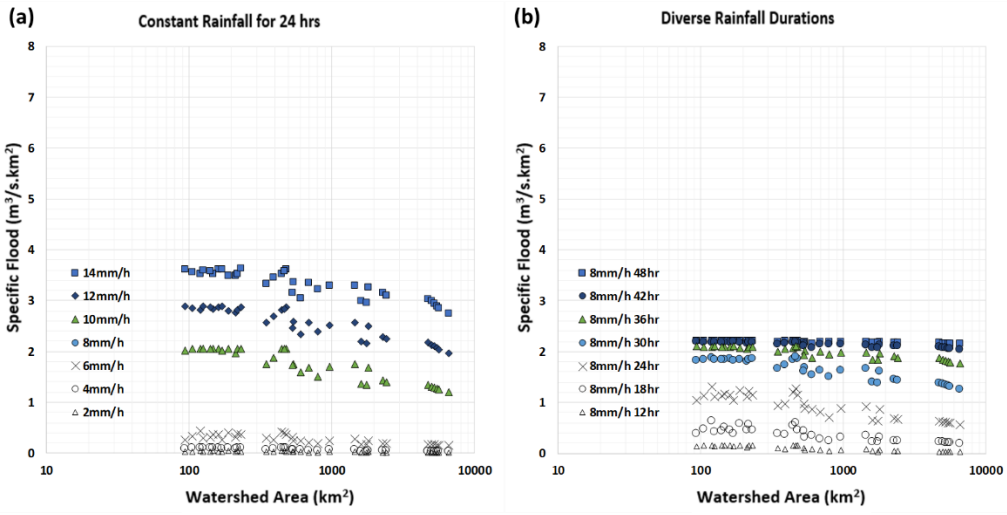

Figure 9. Minimum specific flood dependent on rainfall intensity and rainfall duration.

4.2.2. Rainfall Intensity and Duration

The effects of different sizes of rainfall on the specific flood distribution were investigated in a large watershed. Based on the given ranges of rainfall sizes (i.e., 0–20 mm/h, 4–16 mm/h, and 8–12 mm/h) for 24 h, rainfall sizes were randomly selected and distributed at 35 smaller watersheds. Using randomly selected rainfall values, the Thiessen polygon method provides average rainfall for the CJD watershed. A total of 30 trials were performed within a specified rainfall range in a random rainfall-size-selection manner to ensure specific flood distribution patterns. For comparison purposes, the coefficient of variance (CV) of the rainfall size distribution was applied for each event. Figure 8a–c displays the specific flood of one of the 30 trials, and Figure 8d–f shows the collection of the maximum and minimum specific flood of 30 trials with various ranges of rainfall sizes to show the possible ranges of specific flood for each rainfall range case. Additionally, Figure 8g–i presents the actual events of a specific flood. In the case of 0–20 mm/h (average CV: 59.52), the specific flood distribution displays a widely spread fan shape. If the range of rainfall size is decreased to 8–12 mm/h (average CV: 13.95), the fan shape range is decreased. These results follow the peak discharge distribution trend depending on the spatial CV of total rainfall [6,7]. In Figure 8g–i, the 2013, 2017, and 2002 flood events close to the selected range of rainfall distribution are displayed. The event in 2013 had a wider range of rainfall (CV: 48) and well-distributed rainfall in the CJD watershed. Following the sample patterns of specific floods in Figure 8b,c, the events in 2010 and 2016 have smaller rainfall distribution ranges with smaller CVs of 24.36 and 8.21. From Figure 8, the variances of the specific flood distribution dependent on the variability of rainfall were substantially decreased when the watershed area was larger than 1100 km^2, which is similar to the results of Mandapaka et al. [23], i.e., the basin responses to the variability of rainfall are dampened over 1000 km^2 of watersheds. Based on these results, we can determine the range of rainfall distribution from the diverse sizes of the fan shape in the specific flood distribution.

Another reason for the various sizes of specific floods is diverse rainfall durations with various rainfall intensities. To determine the minimum values of specific floods by providing the range of floods, 24 h rainfall with diverse sizes of rainfall intensity was applied. When diverse sizes of rainfall intensity were applied, each simulation was initially designated with the same size of rainfall intensity (i.e., 2, 4, 6, 8, 12, and 14 mm/h) for 35 smaller watersheds. The selected sizes of rainfall intensities were generally found in actual rainfall observations. Figure 9a shows that the constantly applied rainfall intensity for 24 h generates a horizontally distributed specific flood with some decreased values for larger watershed sizes. The smaller watersheds have a shorter time of concentration, providing a more horizontally straight line. However, larger watersheds require more

time to reach the time of concentration. The time of concentration for a watershed smaller than 450 km^2 was less than 24 h for the CJD watershed, which is approximately within the range of the results of Abdullah et al. [7]. Their results on the relationship between rainfall duration and peak-specific discharge estimated that maximum discharges were obtained for rainfall durations of 5 to 15 h for medium-sized watersheds (200–300 km^2). In Figure 9b, the same rainfall intensity at 8 mm/h was applied for diverse rainfall durations. As previously mentioned, when the time of rainfall duration reached 40 or 48 h, the larger watersheds also had a horizontally straight specific flood distribution, as shown by the smaller watersheds. The size of the specific floods in Figure 9b decreased substantially after 36 h. Ayalew et al. [16] and Furey and Gupta [4] also showed rainfall duration effects on the peak discharge in a power-law relation ($Q(A) = \alpha A^{\theta}$, where $Q(A)$ is the peak discharge, α is the intercept, A is the drainage area, and θ is the exponent. They also mentioned that the increasing rates of intercept and exponent after 36 h were also substantially decreased, similar to our results. Additionally, we found that the increased size of watersheds slowly decreased specific floods, which is different from the real cases (e.g., increased specific flood for larger watersheds, as shown in Figure 8d for the minimum specific flood values). In reality, for many cases, smaller watersheds primarily located upstream often have no rainfall while other locations have rainfall, which can give a specific flood close to zero. Contrarily, the larger watersheds will have some specific flood values because at least some rainfall will be included in the larger area. The reason for the different shapes of the minimum specific flood values is that the simulation has rainfall information for all watersheds. The rainfall intensity is the primary factor that increases the magnitude of a specific flood because Figure 9a shows that the size of a specific flood sensitively increases with the rainfall intensity instead of the rainfall duration [7].

4.3. Ranges of Regional Floods

The envelop curve method was used to establish regional relationships between maximum streamflow data and watershed area using the streamflow data generated at ungauged watersheds. We assumed that the study region is hydroclimatically homogenous, and the size of the watershed area is the primary watershed characteristic controlling the streamflow size [24]. Figure 10 displays the representative regional maximum floods for the CJD watershed. The streamflow data generated using the proposed study were compared with various regional maximum flood equations. Figure 10a shows the applications of Creager's envelope curves [18].

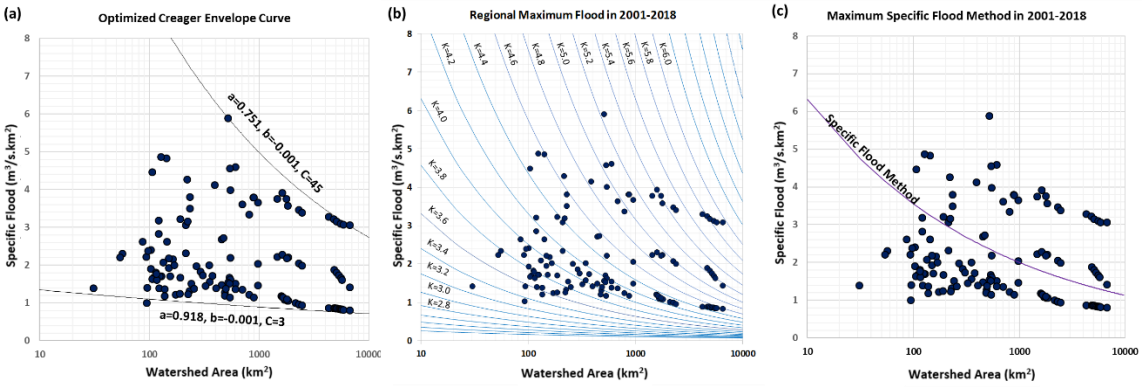

Figure 10. Specific flood for all events with applications of various regional maximum flood equations in 2001–2018. (**a**) Creager's envelop curve, (**b**) Kovacs' regional maximum flood, and (**c**) Korean regional maximum flood).

The upper/lower Creager curve displays the maximum/minimum of the specific flood at each watershed size. The equations of the upper and lower Creager curves use the following values: C = 45, a = 0.751, and b = −0.001; and C = 3, a = 0.918, and b = −0.001, respectively. As shown in Figure 10a, smaller watersheds have a larger variance of a specific

flood because these can be sensitively affected by the various rainfall sizes. However, larger watersheds had little influence on the various rainfall sizes. It is evident that any specific size of the watershed can have an explicit range of specific sizes of floods (e.g., 1–5 $m^3/s \cdot km^2$ for 1000 km^2). Figure 10b shows the Kovacs' regional specific flood equation.

The given specific flood in the CJD watershed can range between K = 3.0 and K = 6.2 in the Kovacs' coefficient to represent the characteristics of watersheds. However, this equation shows the limitation of showing the pattern of the specific flood distribution. Additionally, Figure 10c was plotted using the Korean regional maximum flood equation [19] for a specific flood for the CJD watershed. The specific flood generated for 2001–2009 was not in the range of the maximum floods provided by the KRMF. Therefore, this equation should be modified to be applicable to real cases of specific floods in Korea.

5. Conclusions

The specific flood diagram may have the potential to show the regional streamflow distribution based on the various sizes of floods and watersheds. However, the lack of streamflow data shows the limitation of providing adequate information on streamflow distribution. Thus, the streamflow propagation concept was adopted to provide more spatially distributed streamflow data for ungauged watersheds.

In the process of building a specific flood diagram using the streamflow propagation concept, rainfall information highly influences the distribution patterns of specific floods. The power–law relations were observed to be dependent on the concentrated location of rainfall. If the rainfall is concentrated upstream of the watersheds, the stream located in the same streamline shows a strong power–law profile. A large coefficient variance (CV: 59.52, CV: 13.95) of rainfall intensity ranges reveals a wide fan shape of the specific flood diagram for the smaller watersheds. Rainfall duration and selected size of rainfall were tested for the effects on the minimum values of the specific flood to provide the range of specific floods for diverse watershed sizes. A watershed larger than 450 km^2 requires more time to provide more horizontally distributed minimum values of specific floods. Creager's envelope curve was applied to obtain the maximum and minimum specific flood at various watershed sizes. A watershed size of fewer than 1000 km^2 has a specific range of 1–5 $(m^3/s)(km^2)$. The range of specific floods can be generated for ungauged watersheds of various sizes. Additionally, Kovacs' curve is not suitable for this CJD watershed, and the KRMF must be modified to generate maximum streamflow data for ungauged watersheds. For further study, more rainfall or streamflow data can generalize the range of specific floods for the specified watersheds.

Author Contributions: N.-W.K. and Y.J. conceived and designed the study. K.-H.K. performed calculations. K.-H.K. and Y.J. prepared the original draft. Y.J. supervided the study and revised the manuscript. All authors have read and agreed to the published version of the manuscript.

Funding: This research received no external funding.

Acknowledgments: This study was supported by Wonkwang University in 2021. We are truly grateful for the model support (COSFIM) by K-water in Korea.

Conflicts of Interest: The authors declare no conflict of interest.

References

1. Pegram, G.; Parak, M. A review of the regional maximum flood and rational formula using geomorphological information and observed floods. *Water SA* **2004**, *30*, 377–392. [CrossRef]
2. Kovacs, Z. *Regional Maximum Flood Peaks in Southern Africa*; Technical Report No. 137; Department of Water Affairs: Pretoria, South Africa, 1988.
3. Acreman, M.C. Extreme historical UK Floods and maximum flood estimation. *Water Environ. J.* **1989**, *3*, 404–412. [CrossRef]
4. Furey, P.R.; Gupta, V.K. Effects of excess rainfall on the temporal variability of observed peak-discharge power laws. *Adv. Water Resour.* **2005**, *28*, 1240–1253. [CrossRef]
5. Furey, P.R.; Gupta, V.K. Diagnosing peak-discharge power laws observed in rainfall–runoff events in Goodwin Creek experimental watershed. *Adv. Water Resour.* **2007**, *30*, 2387–2399. [CrossRef]

6. Patnaik, S.; Biswal, B.; Kumar, D.N.; Sivakumar, B. Effect of catchment characteristics on the relationship between past discharge and the power law recession coefficient. *J. Hydrol.* **2015**, *528*, 321–328. [CrossRef]
7. Abdullah, J.; Muhammad, N.S.; Muhammad, S.A.; Julien, P.Y. Envelope curves for the specific discharge of extreme floods in Malaysia. *J. Hydro-Environ. Res.* **2019**, *25*, 1–11. [CrossRef]
8. Sandrock, G.; Viraraghavan, T.; Fuller, G.A. Estimation of peak flows for natural ungauged watersheds in southern Saskatchewan. *Can. Water Resour. J.* **1992**, *17*, 21–31. [CrossRef]
9. McDonnell, J.J.; Beven, K. Debates-The future of hydrological sciences: A (common) path forward? A call to action aimed at understanding velocities, celerities and residence time distributions of the headwater hydrograph. *Water Resour. Res.* **2014**, *50*, 5342–5350. [CrossRef]
10. Merz, R.; Bloschl, G. Regionalisation of catchment model parameters. *J. Hydrol.* **2004**, *287*, 95–123. [CrossRef]
11. Oudin, L.; Andréassian, V.C.; Perrin, C.; Michel, C.; Le Moine, N. Spatial proximity, physical similarity, regression and ungauged catchments: A comparison of regionalization approaches based on 913 French catchments. *Water Resour. Res.* **2008**, *44*, W03413. [CrossRef]
12. Heřmanovský, M.; Havlíček, V.; Hanel, M.; Pech, P. Regionalization of runoff models derived by genetic programming. *J. Hydrol.* **2017**, *547*, 544–556. [CrossRef]
13. Klotz, D.; Herrnegger, M.; Schulz, K. Symbolic Regression for the Estimation of Transfer Functions of Hydrological Models. *Water Resour. Res.* **2017**, *53*, 9402–9423. [CrossRef]
14. Wagener, T.; Wheater, H.S. Parameter estimation and regionalization for continuous rainfall-runoff models including uncertainty. *J. Hydrol.* **2005**, *320*, 132–154. [CrossRef]
15. Kim, N.W.; Jung, Y.; Lee, J.E. Spatial propagation of streamflow data in ungauged watersheds using a lumped conceptual model. *J. Water Clim. Chang.* **2019**, *10*, 89–101. [CrossRef]
16. Ayalew, T.B.; Krajewski, W.F.; Mantilla, R.; Small, S.J. Exploring the effects of hillslope-channel link dynamics and excess rainfall properties on the scaling structure of peak-discharge. *Adv. Water Resour.* **2014**, *64*, 9–20. [CrossRef]
17. Kimura, T. *The Flood Runoff Analysis Method by the Storage Function Model*; The Public Works of Research Institute, Ministry of Construction: Tokyo, Japan, 1961.
18. Creager, W.P.; Justin, J.D.; Hinds, J. *Engineering for Dams*; General Design; John Wiley: New York, NY, USA, 1945; Volume 1.
19. Ministry of Construction. *Report of Water Resource Management in Korea: Guideline of Flood Design Estimation*; Ministry of Construction: Seoul, Korea, 1993.
20. Gupta, V.K.; Mantilla, R.; Troutman, B.M.; Dawdy, D.; Krajewski, W.F. Generalizing a nonlinear geophysical flood theory to medium-sized river networks. *Geophys. Res. Lett.* **2010**, *37*, 11402. [CrossRef]
21. Lima, C.H.R.; Lall, U. Spatial scaling in a changing climate: A hierarchical Bayesian model for non-stationary multi-site annual maximum and monthly streamflow. *J. Hydrol.* **2010**, *383*, 307–318. [CrossRef]
22. Smith, J.A.; Baeck, M.L.; Villarini, G.; Krajewski, W.F. The hydrology and hydrometeorology of flooding in the Delaware River basin. *J. Hydrometeorol.* **2010**, *11*, 841–859. [CrossRef]
23. Mandapaka, P.V.; Krajewski, W.F.; Mantilla, R.; Gupta, V.K. Dissecting the effect of rainfall variability on the statistical structure of peak flows. *Adv. Water Resour.* **2009**, *32*, 1508–1525. [CrossRef]
24. Bayazit, M.; Onoz, B. Envelope curve for maximum floods in Turkey. *Digest* **2004**, 927–931.